

enables real-time data transmission, reception, and control of spacecraft over vast distances. The TTC&M architecture encompasses uplink commands transmitted from ground stations to spacecraft and downlink telemetry and tracking data relayed back to Earth with high reliability, accuracy, and secure encryption. Telemetry provides continuous vital information about spacecraft status, including attitude, thruster performance, and environmental parameters such as temperature, pressure, and subsystem voltage levels [3]. The tracking subsystem determines the spacecraft's trajectory and orbital parameters, while the command subsystem facilitates corrective actions and mission control based on telemetry feedback. Finally, the monitoring subsystem acquires data from on-board scientific instruments and presents it to mission operators at the ground control room. The functional block diagram of entire system is represented in Fig. 1. The frequency spectrum allocation for general telemetry applications is mentioned in Table 1.

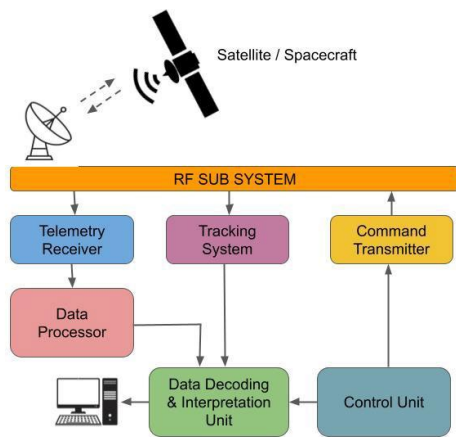


Fig. 1. Block diagram of space telemetry system

Table 1. Frequency spectrum allocation

Frequency Band	Range	Purpose
VHF	137-174 MHz	Weather forecasting
UHF	400-470 MHz	Telemetry Beacons
L	1.2 – 1.5 GHz	Aircraft Telemetry
S	2.2 – 2.3 GHz	Space Telemetry
C	4.4 – 5.0 GHz	Missile telemetry
X	8.0 – 12.0 GHz	Deep Space Network
Ka	26.5 – 40 GHz	Cross Link Network

(Source: <https://www.slideshare.net/slideshow/ttc-subsystem/232524997>)

The key block of space telemetry system is the RF subsystem, which composed of microwave oscillators, RF amplifiers, antenna units, and associated matching networks. The operational frequencies of generalized telemetry systems range from the Very High Frequency (VHF) and Ultra High Frequency (UHF) bands up to the lower sub-millimeter wave region. While VHF and UHF bands are widely utilized for weather forecasting and near-earth telemetry beacon applications, their susceptibility to ionospheric distortion makes them not suitable for deep

space missions. The S-band and X-band frequencies are preferred for most space telemetry operations due to their superior ionospheric transparency, lower atmospheric absorption, and broader bandwidth characteristics [4]. Although millimeter-wave frequencies suffer from increased propagation loss, they are being increasingly considered for high-capacity satellite cross-links and data backhaul in next-generation space communication networks [5]

This paper presents detailed analysis of the key challenges in space telemetry systems, including atmospheric attenuation, signal latency, Doppler shift, spectrum allocation, and power management constraints. It also highlights emerging advancements in antenna technologies such as high gain parabolic reflectors, specialized microstrip antennas, and adaptive phased array systems that are widely used in modern space telemetry systems. Furthermore, the paper provides a comparative evaluation of various antenna configurations used in space telemetry, highlighting their performance metrics and mission specific suitability. The section concludes with a comprehensive comparison of these antenna systems in terms of gain, bandwidth, beam steering capability, efficiency, and structural adaptability.

2. CHALLENGES IN SPACE TELEMETRY

Although space communication technology has advanced greatly, developing reliable telemetry systems still suffer from several critical challenges. These challenges primarily arise due to the harsh conditions of the space environment, the long propagation distances involved, and the limitations of available power and spectrum resources. The major issues affecting the performance of space telemetry systems are discussed below.

A. Atmospheric Attenuation

Atmospheric attenuation is a major factor that directly influencing signal degradation, particularly in the upper microwave frequency ranges. The signal absorption due to atmospheric gases such as oxygen and water vapour molecules leads to substantial path losses, especially in the frequency bands above 10 GHz [6]. The effect becomes more severe during harsh weather conditions, including heavy rain and extreme humidity envelopments, which can cause amplitude fading and reduce link reliability. Therefore, appropriate frequency band selection and adaptive power control are essential to compensate these effects.

B. Signal Latency

In deep space missions, communication links can extend over huge distances, resulting in significant signal propagation delays. This latency severely limits real time command and control operations, necessitating the use of autonomous on board systems capable of executing time-critical tasks without immediate ground intervention [7].

C. Doppler Shift

Relative motion between the spacecraft and ground station introduces Doppler shifts in the received signal frequency. This shift may affect carrier recovery, bit synchronization, and decoding processes, especially for high data rate communication links. Advanced frequency tracking systems are required to maintain link integrity under varying Doppler conditions [8].

D. Thermal and Radiation Effects

Electronic components in space telemetry systems are exposed to extreme temperature variations and ionizing radiation, which can degrade amplifier efficiency, oscillator stability, and antenna performance. Radiation-induced bit errors and device failures further affect telemetry data integrity. Implementation of radiation-hardened components, redundant subsystems, and error-correcting codes is therefore vital for long-term mission reliability [9].

E. Spectrum Allocation

The growing demand of space missions has led to congestion in traditionally used telemetry frequency bands such as S-band and X-band. The limited availability of dedicated spectrum resources may lead to interference [10]. Efficient spectrum utilization, dynamic allocation, and transition toward higher frequency bands are good choices to overcome this constraint.

F. Power Constraints

Power resources availability of the spacecraft is very limited, particularly for small satellites and deep space probes. Since transmission power directly affects link quality, achieving sufficient signal-to-noise ratio (SNR) over vast distances becomes a major concern. High-efficiency RF amplifiers, directional high-gain antennas, and power optimized

modulation schemes are essential for maintaining communication performance under stringent power budgets [11].

3. SPACE TELEMETRY ANTENNAS

To overcome the challenges associated with deep space communication, it is essential to employ a highly efficient antenna system that satisfies the performance specifications. The main requirements for space telemetry system include high gain and directivity for long range communication, low side lobe levels to reduce interference, and the ability to steer the beam towards the direction as required for accurate tracking. Among the various antenna configurations, the parabolic reflector antenna is the most widely used in deep space missions. It provides extremely high gain towards the direction of propagation, making it ideal for transmitting and receiving weak signals over vast distances. The microstrip antenna is preferred for its compactness, light weight, and less effort to integrate with satellite structures. The phased array antenna is another advanced solution, offering electronic beam steering without physical movement. The following section discusses the specific antenna type in detail.

A. Parabolic Reflector Antenna

The parabolic reflector antenna is commonly employed at ground stations to maintain continuous communication with spacecraft. Its key characteristics include high gain, directivity, and the capability to mechanically steer the beam over a wide coverage area in the space. A 70-meter parabolic reflector antenna, DSS-14, as shown in Fig. 2(a), also known as the Goldstone Antenna, is operated by NASA's Deep Space Network (DSN) and plays a vital role in telemetry and communication for NASA's deep space missions [12]. It supports S-band (2.2 - 2.3 GHz), X-band (7.1 - 8.4 GHz), and Ka-band (31.8 - 32.3 GHz) frequencies, ensuring reliable deep space communication. The system is capable of transmitting up to 400 kW of peak RF power and employs Cryogenically Cooled Low Noise Amplifiers (CCLNA) for the reception of extremely weak signals from distant spacecraft. Similarly, a 35-meter antenna located at New Norcia [13], Western Australia, as shown in Fig. 2(b), serves as part of the European Space Agency's (ESA) deep space communication network. It supports S-band (2.2 - 2.3 GHz), X-band (7.1 - 8.4 GHz), and Ka-band (31.8 - 32.3 GHz) frequencies, with a peak

transmission power of 20 kW, and is also equipped with a CCLNA system for sensitive signal reception. In India, the Indian Deep Space Network (IDSN), as shown in Fig. 2(c), comprises a 32-meter parabolic antenna located near Bengaluru. It supports S-band (2.2 - 2.3 GHz) and X-band (7.1 - 8.4 GHz) frequencies and is equipped with a 20 kW transmitter along with CCLNA based receiver systems for deep space telemetry and command operations [14].

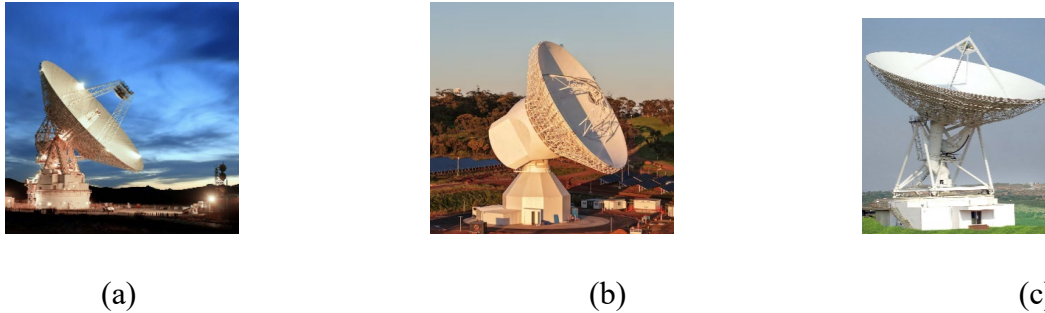


Fig. 2. Deep space antennas (a) DSS-14 NASA (b) DSA -1 ESA (c) ISDN – ISRO.

(Source: (a) <https://www.nasa.gov/communicating-with-missions/dsn/> (b) https://www.esa.int/Enabling_Support/Operations/ESA_inaugurates_deep_space_antenna_in_Australia (c) <https://www.aerospaceinindia.org/idsn-campus/>)

B. Specialized Microstrip Antennas

Microstrip antennas offer a compact form factor, low weight, and ease of integration with active components such as microwave switching elements and amplifiers directly on the surface. Furthermore, they are well suited for deployment in small payloads. In contrast, bulky parabolic reflector antennas are often unsuitable for space missions where power consumption, size, and payload weight are critical constraints [15]. Under such conditions, specialized microstrip antennas become more suitable. These antennas differ from conventional microstrip designs by exhibiting higher gain, reduced back-lobe and side-lobe levels, minimal loss at the target frequencies, and support for multiple operating bands in a single antenna structure. A circularly polarized (CP) S-band microstrip antenna for satellite telemetry applications was presented in [16]. The antenna structure consists of two sets of stacked patch antennas, as illustrated in Fig. 3(a), enabling both left-hand circular polarization (LHCP) and right-hand circular polarization (RHCP). The proposed design achieves a wide impedance bandwidth of 300 MHz, effectively covering the 2.0–2.3 GHz frequency range, with

a peak gain of 6 dBi. The return loss characteristics and radiation pattern of the proposed antenna are shown in Fig. 3(b) and Fig. 3(c), respectively.

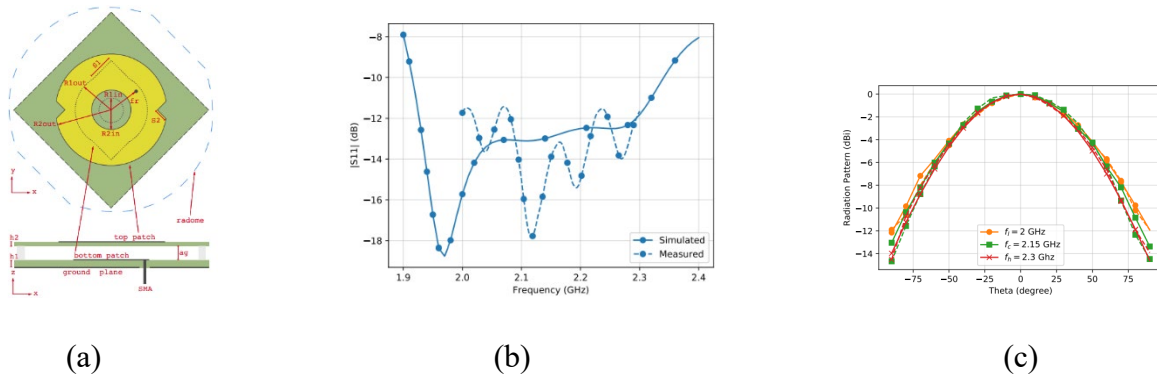


Fig. 3. CP S-Band antenna (a) structure (b) return loss(S_{11}) (c) Radiation pattern.

(Source: Squadrito, P., Livreri, P., Di Donato, L., Squadrito, C., & Sorbello, G. (2019). A Telemetry, Tracking, and Command Antennas System for Small-Satellite Applications. *Electronics*, 8(6), 689. <https://doi.org/10.3390/electronics8060689>.)

A compact multiband microstrip patch antenna for C, X, and Ku-band satellite applications is presented in [17]. The proposed design consists of a pentagon-shaped radiating patch with four circular structures placed at each corner, as shown in Fig. 4(a). This geometry is selected to achieve multiple resonant frequencies. A partial ground plane is used to enhance the bandwidth and maximize the gain. Additionally, cross-shaped elements are incorporated within the patch to further improve the overall antenna performance. The proposed antenna operates at 7.6 GHz and 12 GHz, achieving peak gains of 7.13 dBi and 8.07 dBi, respectively. The return loss characteristics and radiation patterns of the antenna are shown in Fig. 4(b) and Fig. 4(c).

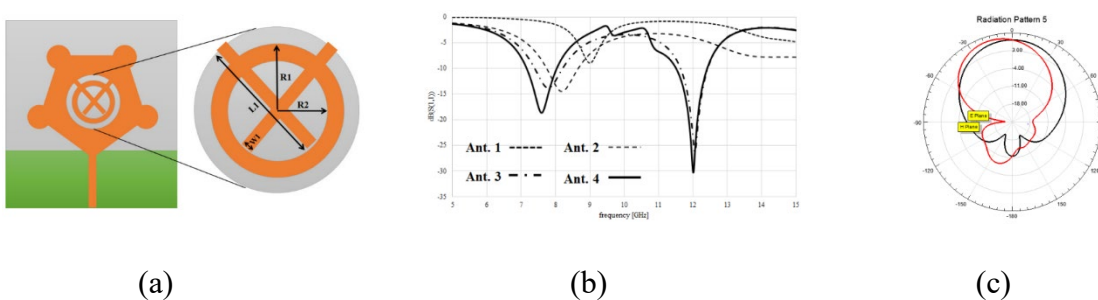


Fig. 4. Multi band patch antenna (a) structure (b) return loss(S_{11}) (c) Radiation pattern.

(Source: Zahid, M., Taqdeer, M. M., & Amin, Y. (2023). *A Compact Dual-Band Microstrip Patch Antenna for C- and X- and Ku-Band Applications*. *Engineering Proceedings*, 46(1), 16. <https://doi.org/10.3390/engproc2023046016>.)

An electromagnetic band gap (EBG)-based X-band antenna for CubeSat applications was reported in [18]. The EBG structure comprises periodically arranged metallic patch elements that behave as a resonant LC circuit at specific frequencies, thereby enhancing antenna gain through the resonance. The proposed configuration employs a single-layer EBG ring surrounding the main radiator element, as illustrated in Fig. 5(a). To achieve right-hand circular polarization (RHCP), the primary radiator incorporates diagonally oriented square slots, which excite two orthogonal modes with a 90° phase difference. The antenna exhibits a peak gain of 11.7 dBi and a radiation efficiency of approximately 95% at the operating frequency of 8.48 GHz. The return loss characteristics and radiation patterns of the antenna are presented in Fig. 5(b) and Fig. 5(c), respectively.

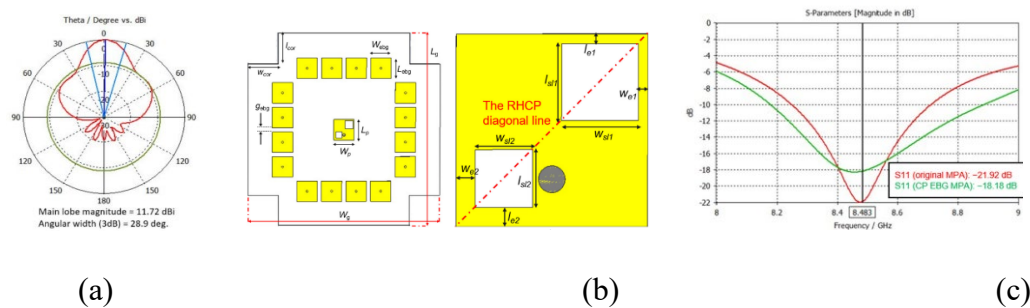


Fig. 5. EBG antenna (a) structure (b) return loss(S_{11}) (c) Radiation pattern.

(Source: Ta, L. P., Nakayama, D., & Hirose, M. (2025). *Design of a High-Gain X-Band Electromagnetic Band Gap Microstrip Patch Antenna for CubeSat Applications*. *Electronics*, 14(11), 2216. <https://doi.org/10.3390/electronics14112216>.)

C. Phased Array Antennas

Phased array antennas can support electronic beam steering capability, and rapid reconfigurability without any mechanical systems. Their compact structure and high power capabilities make them suitable for integration into modern space communication and navigation systems [19]. The beam steering mechanism is realized by electronically controlling

the phase of the radiated electromagnetic waves using a phase shifter unit. An S-band microstrip phased-array antenna, specifically designed for ground station tracking applications, is presented in [20]. The antenna system comprises 16 subarrays, 16 beamforming RF modules, a power control board, and a 16-way feed network, as illustrated in Fig. 6(a). Each subarray, formed by combining two 8×1 arrays, achieved a gain of 16.1 dBi and a reflection coefficient better than -10 dB across the 2.12–2.45 GHz frequency range. The antenna supports a beam scanning range of -20° to $+20^\circ$. The return loss characteristics and radiation patterns are shown in Figs. 6(b) and 6(c), respectively.

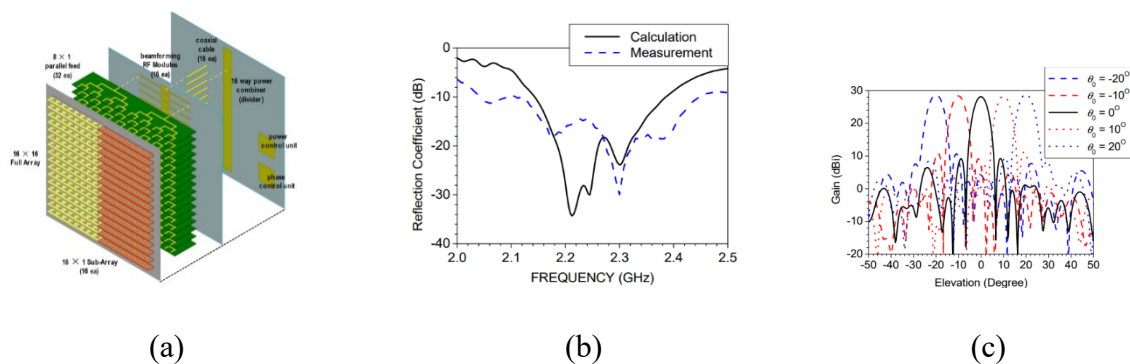


Fig. 6. Multi layer phased array antenna (a) structure (b) return loss(S_{11}) (c) Radiation pattern.

(Source: Robert Mailloux, *Phased Array Antenna Handbook, Third Edition*, Artech, 2017.)

Microstrip array based phased-array antennas are not suitable for very high-power applications. In such cases, waveguide-based antenna systems are preferred, as they can offer higher gain, directivity and able to handle several thousand watts of power [21]. A study reported in [22] presents such a system, comprising an 8×1 phased-array unit, as illustrated in Fig. 7(a). Each unit includes a horn antenna integrated with an active phase-shifter mechanism to achieve beam steering toward the desired direction. The antenna operates within the 7.5–8.5 GHz frequency range, achieving a peak gain of 27.9 dBi and a maximum power-handling capacity of 56.34 MW. It supports beam scanning from -10° to $+10^\circ$. The return loss characteristics and radiation patterns are presented in Figs. 7(b) and 7(c), respectively.

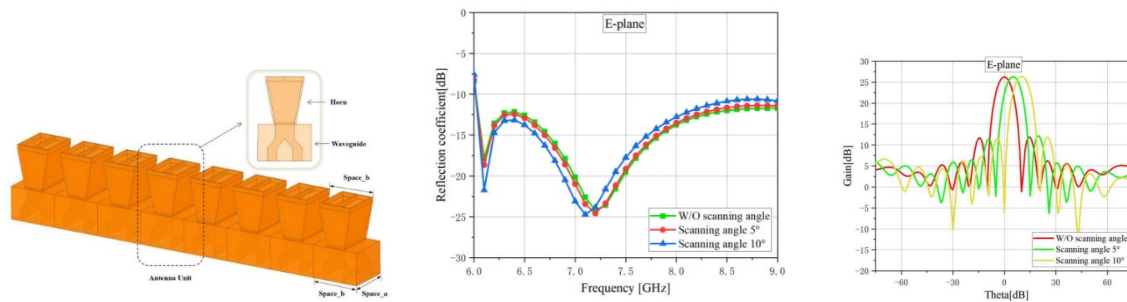


Fig. 7. Waveguide phased array antenna (a) structure (b) return loss(S_{11}) (c) Radiation pattern.

(Source: Liu, R., Wang, N., Li, T., Zhang, R., & Wu, H. (2022). *X-Band Active Phased Array Antenna Using Dual-Port Waveguide for High-Power Microwave Applications*. *Electronics*, 11(23), 4064. <https://doi.org/10.3390/electronics11234064>.)

4. FUTURE RESEARCH DIRECTIONS

The continuous research and development of space telemetry and communication systems opens lot of opportunities for adaptive, high-efficiency, and intelligent antenna systems. Future studies can focus on reconfigurable phased-array architectures that dynamically alter their operating frequency, polarization, and beam direction to maintain robust communication under harsh space conditions. The integration of AI driven beamforming algorithms and machine learning based signal optimization could further enhance link reliability, interference mitigation, and autonomous calibration in deep space networks [23]. In addition, the development of hybrid antenna systems that combine the advantages of parabolic reflectors, microstrip arrays, waveguide structures, and pixel antennas may enable scalable and flexible solutions suitable for deep space missions. The pixel antenna concept, where an array of small radiating elements (pixels) can be electronically reconfigured to change aperture geometry and radiation patterns offers significant potential for real time beam reconfiguration, polarization shifting, and enables multi band operation [24]. This approach allows for high adaptability without mechanical movement, making it particularly attractive for compact satellite payloads and multi-mission spacecraft requiring versatile communication links. Moreover, research into radiation hardened materials, additive manufacturing techniques, and

metamaterial based substrates is expected to further improve thermal endurance, reduce mass, and enhance gain stability under harsh radiation environments. The integration of these advanced materials with pixel based and phased array architectures could open the way for next generation intelligent space antennas, capable of self-healing, self-calibration, and autonomous optimization to ensure continuous high-quality communication in deep space.

5. COMPREHESIVE SUMMERY

This section provides a comprehensive summary of the reported literature, presented in Table 2. The table outlines the antenna structure and type, operating frequency band, achieved gain, and proposed applications.

Table 2. Comprehensive summary of literature.

Ref	Antenna Structure	Antenna Type	Operating Frequency Bands (Band / GHz)	Peak Gain (dBi)	Applications
[12]	Goldstone DSS-14(NASA)	Parabolic Reflector	S (2.2 - 2.3) X (7.1 - 8.4) Ka (31.8 - 32.3)	85	Deep space telemetry, Satellite tracking
[13]	DSA – 1 (ESA)	Parabolic Reflector	S (2.2 - 2.3) X (7.1 - 8.4) Ka (31.8 - 32.3)	80	Deep space telemetry, Satellite tracking
[14]	ISDN (ISRO)	Parabolic Reflector	S (2.2 - 2.3) X (7.1 - 8.4)	78	Deep space telemetry, Satellite tracking
[16]	S - Band CP Antenna	Microstrip	S (2.0 - 2.3)	6	CP antenna for Satellite telemetry
[17]	Multi Band Patch Antenna	Microstrip	X & Ku (7.6-12.2)	8.07	Multi band satellite communication

[18]	EBG Antenna	Microstrip	X (8.48)	11.7	Cube sat point to point communication
[20]	Multilayer phased Array Antenna	Phased array	S (2.12 – 2.45)	16.1	Space telemetry and Radar Navigation
[22]	Waveguide phase Array Antenna	Phased array	X (7.5 – 8.5)	27.9	Space telemetry and Radar Navigation

6. CONCLUSION

The high demand of space telemetry and communication systems continues to develop innovations in antenna technology, enabling reliable long distance data exchange across extreme environments. This review has examined the fundamental challenges including atmospheric attenuation, Doppler effects, spectrum resource allocation, and power constraints that affect telemetry system performance. It has also discussed the comparative characteristics and advantages of parabolic reflectors, microstrip antennas, and phased array configurations for various mission scales. Recent developments in adaptive and intelligent antenna architectures, supported by advances in AI-driven beamforming, metamaterial substrates, and additive manufacturing, are opening the way for next generation space communication networks. The integration of these technologies promises higher gain, lower weight, and enhanced radiation characteristics, essential for deep space missions.

REFERENCES

- [1] C. G. Christodoulou, Y. Tawk, S. A. Lane and S. R. Erwin, "Reconfigurable Antennas for Wireless and Space Applications," in *Proceedings of the IEEE*, vol. 100, no. 7, pp. 2250-2261, July 2012, doi: 10.1109/JPROC.2012.2188249.
- [2] A. Modenini and B. Ripani, "A Tutorial on the Tracking, Telemetry, and Command (TT&C) for Space Missions," in *IEEE Communications Surveys & Tutorials*, vol. 25, no. 3, pp. 1510-1542, thirdquarter 2023, doi: 10.1109/COMST.2023.3287431.

- [3] Y. Zhan, P. Wan, C. Jiang, X. Pan, X. Chen and S. Guo, "Challenges and Solutions for the Satellite Tracking, Telemetry, and Command System," in *IEEE Wireless Communications*, vol. 27, no. 6, pp. 12-18, December 2020, doi: 10.1109/MWC.001.2000089.
- [4] Z. Sun, *Technologies for Deep Space Exploration*. Singapore: Springer Nature, 2020.
- [5] J. Bang, H. Chung, J. Hong, H. Seo, J. Choi and S. Kim, "Millimeter-Wave Communications: Recent Developments and Challenges of Hardware and Beam Management Algorithms," in *IEEE Communications Magazine*, vol. 59, no. 8, pp. 86-92, August 2021, doi: 10.1109/MCOM.001.2001010.
- [6] G. Marner, "Atmospheric attenuation of microwave radiation," *1958 IRE International Convention Record*, New York, NY, USA, 1955, pp. 68-71, doi: 10.1109/IRECON.1955.1150299.
- [7] B. Soret, S. Ravikanti and P. Popovski, "Latency and timeliness in multi-hop satellite networks," *ICC 2020 - 2020 IEEE International Conference on Communications (ICC)*, Dublin, Ireland, 2020, pp. 1-6, doi: 10.1109/ICC40277.2020.9149009.
- [8] Y. A. Ahmad, T. S. Gunawan, A. I. A. Rahman, H. H. A. Shukur, H. Sanusi and N. M. Yusoff, "Doppler Shift Analysis for Enhanced Satellite Communication in Low Earth Equatorial Orbits," *2024 IEEE 10th International Conference on Smart Instrumentation, Measurement and Applications (ICSIMA)*, Bandung, Indonesia, 2024, pp. 92-97, doi: 10.1109/ICSIMA62563.2024.10675552.
- [9] A. Y. Alhilal, T. Braud and P. Hui, "A Roadmap Toward a Unified Space Communication Architecture," in *IEEE Access*, vol. 9, pp. 99633-99650, 2021, doi: 10.1109/ACCESS.2021.3094828.
- [10] E. C. Stone, "Communications technologies for space exploration," in *Proceedings of the IEEE*, vol. 87, no. 6, pp. 1044-1046, June 1999, doi: 10.1109/5.763318.
- [11] M. S. Gatti, M. J. Klein and T. B. H. Kuiper, "The Goldstone 70-meter antenna performance at 32 GHz," *International Symposium on Antennas and Propagation Society*,

Merging Technologies for the 90's, Dallas, TX, USA, 1990, pp. 1329-1332 vol.3, doi: 10.1109/APS.1990.115358.

[12] R. Martin and M. Warhaut, "ESA's 35-meter Deep Space Antennas at New Norcia/Western Australia and Cebreros/Spain," *2004 IEEE Aerospace Conference Proceedings (IEEE Cat. No.04TH8720)*, Big Sky, MT, USA, 2004, pp. 1124-1133 Vol.2, doi: 10.1109/AERO.2004.1367713.

[14] A. A. Bhardwajan, A. Arora, S. Dakkumalla, F. Ahmed and T. S. Ganesh, "Precise Time and frequency dissemination to Indian Deep Space Network from NavIC PTF," *2021 XXXIVth General Assembly and Scientific Symposium of the International Union of Radio Science (URSI GASS)*, Rome, Italy, 2021, pp. 1-3, doi: 10.23919/URSIGASS51995.2021.9560118.

[15] D. M. Pozar, "Microstrip antennas," in *Proceedings of the IEEE*, vol. 80, no. 1, pp. 79-91, Jan. 1992, doi: 10.1109/5.119568.

[16] Squadrito, P., Livreri, P., Di Donato, L., Squadrito, C., & Sorbello, G. (2019). A Telemetry, Tracking, and Command Antennas System for Small-Satellite Applications. *Electronics*, 8(6), 689. <https://doi.org/10.3390/electronics8060689>.

[17] Zahid, M., Taqdeer, M. M., & Amin, Y. (2023). A Compact Dual-Band Microstrip Patch Antenna for C- and X- and Ku-Band Applications. *Engineering Proceedings*, 46(1), 16. <https://doi.org/10.3390/engproc2023046016>.

[18] Ta, L. P., Nakayama, D., & Hirose, M. (2025). Design of a High-Gain X-Band Electromagnetic Band Gap Microstrip Patch Antenna for CubeSat Applications. *Electronics*, 14(11), 2216. <https://doi.org/10.3390/electronics14112216>.

[19] Robert Mailloux, *Phased Array Antenna Handbook, Third Edition*, Artech, 2017.

[20] S. Li et al., "S-band phased array antenna for satellite ground station tracking," *IEEE Access*, vol. 11, pp. 119433–119441, 2023.

[21] Lee, D.-H., Seo, J.-W., Lee, M.-S., Chung, D., Lee, D., Bang, J.-H., Satriyotomo, B., & Pyo, S. (2022). An S-Band-Receiving Phased-Array Antenna with a Phase-Deviation-

Minimized Calibration Method for LEO Satellite Ground Station Applications. *Electronics*, 11(23), 3847. <https://doi.org/10.3390/electronics11233847>.

[22] Liu, R., Wang, N., Li, T., Zhang, R., & Wu, H. (2022). X-Band Active Phased Array Antenna Using Dual-Port Waveguide for High-Power Microwave Applications. *Electronics*, 11(23), 4064. <https://doi.org/10.3390/electronics11234064>.

[23] M. O. Akinsolu, Q. Hua and B. Liu, "Automated Design of Antennas Using AI Techniques: A Review of Contemporary Methods and Applications," *2024 18th European Conference on Antennas and Propagation (EuCAP)*, Glasgow, United Kingdom, 2024, pp. 1-4, doi: 10.23919/EuCAP60739.2024.10500986.

[24] S. Shen, K. -K. Wong and R. Murch, "Antenna Coding Empowered by Pixel Antennas," in *IEEE Transactions on Communications*, doi: 10.1109/TCOMM.2025.3621089.